37. R. E. Warner, *Condor* **70**, 101 (1968); I. A. E. Atkinson, in *Conservation of Island Birds: Case Studies for the Management of Threatened Island Species*, P. J. Moors, Ed. (International Council for Bird Preservation, Cambridge, 1985), p. 35; P. W. Price, M. J. Westoby, B. Rice, *Am. Nat.* **131**, 544 (1988); R. N. Mack, in (*37*, p. 155).
38. J. A. Drake *et al.*, Eds., *Biological Invasions: a Global Perspective* (Wiley, Chichester, 1989).
39. D. S. Simberloff in, *Biotic Crises in Ecological and Evolutionary Time*, M. H. Nitecki, Ed. (Academic Press, New York, 1981), p. 53; J. M. Diamond, in *Quaternary Extinctions: a Prehistoric Revolution* (Univ. of Arizona Press, Tucson, 1984), p. 824.
40. G. J. Vermeij and E. J. Petuch, *Malacologia* **27**, 29 (1986).
41. G. J. Vermeij, *Conserv. Biol.* **3**, 274 (1989); *Paleobiology* **15**, 335 (1989).
42. G. J. Vermeij, *Evolution and Escalation, an Ecological History of Life* (Princeton Univ. Press, Princeton, 1987); M. H. Rosenzweig and R. D. McCord, *Paleobiology*, in press.
43. P. K. Dayton, *Ecol. Monogr.* **41**, 351 (1971); H. S. Horn, *The Adaptive Geometry of Trees* (Princeton Univ. Press, Princeton, 1971); J. P. Sutherland, *Am. Nat.* **108**, 859 (1974); J. H. Connell, *Science* **199**, 1302 (1978); R. T. Paine and S. A. Levin, *Ecol. Monogr.* **51**, 145 (1981).
44. A. Hallam, in *Causes of Evolution: a Paleontological Perspective* (Univ. of Chicago Press, Chicago, 1990), p. 249.
45. V. Geist, *Wildl. Soc. Bull.* **13**, 351 (1985).
46. W. J. Christie, *J. Fish. Res. Board Canada* **31**, 827 (1974); J. M. Diamond and C. R. Veitsch, *Science* **211**, 499 (1981); M. D. Fox and B. J. Fox, in *Ecology of Biological Invasions*, R. H. Groves and J. J. Burdon, Eds. (Cambridge Univ. Press, Cambridge, 1986), p. 57.
47. J. Roughgarden, *Evolution* **41**, 1130 (1987); S. L. Pimm, in (*37*, p. 351); T. J. Case, *Proc. Nat. Acad. Sci. U.S.A.* **87**, 9610 (1990).
48. A. R. Wallace, *The Geographical Distribution of Animals* (Hafner, New York, 1876).
49. T. M. Zaret and R. T. Paine, *Science* **182**, 449 (1973); J. A. Savidge, *Ecology* **68**, 660 (1987); J. Murray, E. Murray, M. S. Johnson, B. Clarke, *Pac. Sci.* **42**, 150 (1988); J. H. Brown, in (*37*, p. 85).
50. D. W. Krause, *Contrib. Geol. Univ. Wyo. Spec. Pap.* **3**, 95 (1986); M. C. Maas, D. W. Krause, S. G. Strait, *Paleobiology* **14**, 410 (1988).
51. M. Ben-Yami and T. Glaser, *Fish. Bull.* **72**, 359 (1974); M. D. Bertness, *Ecology* **65**, 370 (1984); M. B. Usher, *Biol. Conserv.* **44**, 119 (1988).
52. N. W. Blackstone, *Biol. Bull.* **171**, 379 (1986); M. H. Posey, *Mar. Ecol. Prog. Ser.* **31**, 15 (1986); P. M. Vitousek, L. R. Waller, L. D. Whiteaker, D. Mueller-Dombois, P. A. Matson, *Science* **238**, 802 (1987).
53. R. H. MacArthur, *Geographical Ecology: Patterns in the Distribution of Species* (Harper & Row, New York, 1972); R. H. Whittaker, *Evol. Biol.* **10**, 1 (1977); P. W. Price, *Evolutionary Biology of Parasites* (Princeton Univ. Press, Princeton, 1980); K. Rohde, *Evol. Theory* **8**, 305 (1989). Many vertebrate assemblages are probably well below saturation [see also J. A. Wiens, *The Ecology of Bird Communities, Foundations and Patterns* (Cambridge Univ. Press, Cambridge, 1989), vol. 1].
54. M. D. Bertness, *J. Exp. Mar. Biol. Ecol.* **64**, 159 (1982); G. J. Vermeij, *Mar. Ecol. Prog. Ser.* **57**, 293 (1989).
55. J. C. Briggs, *Science* **162**, 511 (1968).
56. R. W. Topp, *ibid.* **165**, 1325 (1969).
57. I thank J. Cooper, E. Zipser and J. Fong for technical assistance and P. K. Dayton, E. G. Leigh, J. F. Quinn, A. Shapiro, and P. W. Signor for critically reading the manuscript.

Vapor-Phase Fabrication and Properties of Continuous-Filament Ceramic Composites

T. M. BESMANN, B. W. SHELDON,* R. A. LOWDEN, D. P. STINTON

The continuous-filament ceramic composite is becoming recognized as necessary for new, high-temperature structural applications. Yet because of the susceptibility of the filaments to damage from traditional methods for the preparation of ceramics, vapor-phase infiltration has become the fabrication method of choice. The chemical vapor infiltration methods for producing these composites are now being studied in earnest, with the complexity of filament weaves and deposition chemistry being merged with standard heat and mass-transport relationships. Two of the most influential effects on the mechanical properties of these materials are the adhesion and frictional force between the fibers and the matrix, which can be controlled by a tailored interface coating. A variety of materials are available for producing these composites including carbide, nitride, boride, and oxide filaments and matrices. Silicon carbide–based materials are by far the most advanced and are already being used in aerospace applications.

UNTIL JUST A FEW YEARS AGO, VAPOR-PHASE SYNTHESIS was rarely thought of as a route to structural materials.The technology was restricted to the deposition of specialty coatings and, more recently, to the fabrication of thin-film electronic devices. Now, however, it is emerging as a method for the preparation of near-final-shape, continuous-filament ceramic composites (CFCCs) for advanced structural applications. Conventional techniques for the fabrication of ceramics such as hot pressing (in which a ceramic body is simultaneously subjected to high temperatures and pressures) involve fiber-damaging extremes of temperature and mechanical stress. For example, the popular SiC-based fiber Nicalon suffers degradation at processing temperatures above 1100°C (*1, 2*), a temperature well below that for sintering SiC. The high-modulus, small-diameter (15-μm) Nicalon fibers are also susceptible to mechanical damage from high-pressure consolidation methods. This susceptibility has led to several novel approaches involving impregnation of fibrous preforms with matrix precursors. By far the greatest success has been obtained with vapor sources, leading to a class of techniques termed chemical vapor infiltration (CVI).

CVI originated in efforts to densify porous graphite bodies by infiltration with carbon (*3*). The technique has developed commercially such that half of the carbon-carbon composites currently produced are made by CVI (the remainder are fabricated by the curing of polymer-impregnated fiber lay-ups). The earliest report of the use of CVI for ceramics fabrication was a 1964 patent for infiltrating fibrous alumina with chromium carbides (*4*). During the past two decades, much of the development of CVI techniques has taken place at the University of Karlsruhe (*5*), the University of Bordeaux (*6*), and Oak Ridge National Laboratory (*7, 8*).

In CVI, gaseous reactants infiltrate a porous (typically fibrous) preform held at an elevated temperature, depositing matrix material on the substrate structure via a standard chemical vapor deposition (CVD) reaction. This CVD coating grows with continued deposition to form the composite matrix. CVD reactions are attractive in that they permit the use of a wide variety of ceramic matrix materials

---

The authors are at Oak Ridge National Laboratory, Post Office Box 2008, Oak Ridge, TN 37831-6063.

*Currently at the Division of Engineering, Brown University, Box D, Providence, RI 02912.

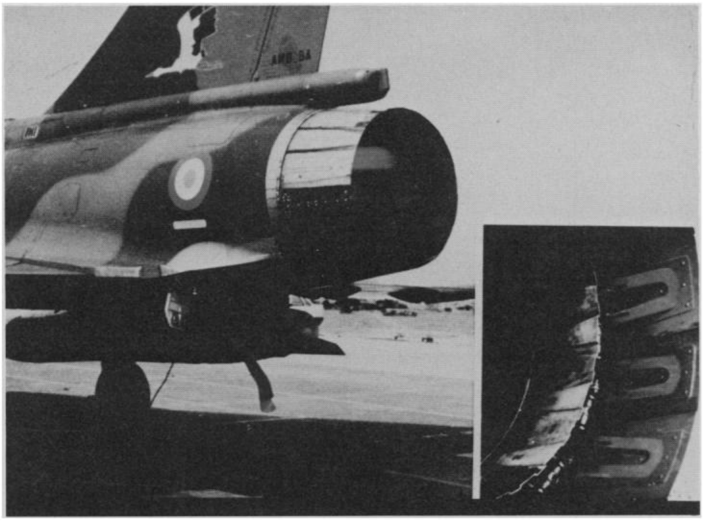

Fig. 1. Mirage aircraft thrust deflector fabricated by CVI.

including silicides, borides, carbides, nitrides, and oxides. Another advantage of CVD is that it allows the formation of very high melting point materials at relatively low temperatures, sparing the fibers from degradation. An excellent example of a high-temperature matrix material is TiB_2, which has a melting point of 3225°C but which can be easily deposited at 900°C via

$$TiCl_4 + 2BCl_3 + 5H_2 \rightarrow TiB_2 + 10HCl \quad (1)$$

CVI also imposes little mechanical stress on the fibers, and proper tailoring of the fiber-interface-matrix system together with only modest differences in thermal expansion coefficients produce a CFCC with minimal residual stress.

The demand for structural ceramics such as the CFCCs has grown substantially in the past decade and has led to the rapidly expanding interest in CVI. CFCCs have been developed in response to requirements for lighter, stronger, more corrosion-resistant materials capable of performing at higher temperatures. The National Research Council has cited such advanced materials as crucial to the growth, prosperity, and economic well-being of U.S. industry (*9*). The potential uses of ceramics range from heat engines to tool bits to aerospace components. Penetration of these markets by traditional ceramics has been extremely limited, however, because of their characteristic brittleness (low toughness) and high sensitivity to flaws, which result in expensive component testing and a high rejection rate. Attention has thus focused on ceramic composites that have demonstrated significantly greater toughness than monolithics and are relatively flaw-insensitive (*10*).

Ceramics can be toughened by the addition of a variety of second phases (for example, whiskers, platelets) that act to blunt cracks and, for fibers or whiskers, absorb crack energy through pullout from the matrix. CFCCs have continuous ceramic fibers embedded in the ceramic matrix. The fibers reinforce the ceramic to create a composite that is several times as tough as the unreinforced ceramic. The composite can be fabricated into near-net-shape products if the fibers are woven into the shape of the final component before matrix infiltration. The great value of CFCCs is the ability to design components such that the fibers trace the strain lines. One of the first products so designed and produced is a CFCC thrust deflector currently used in French Mirage jets (Fig. 1).

In a CFCC, a high-strength, relatively brittle fiber is used to reinforce a brittle matrix. In contrast to polymer or metal matrix composites—or even many of the glass matrix composites—the modulus of the reinforcement can be lower than that of the matrix, and the strain to failure of the fibers is generally higher than that of the matrix. CFCCs may not be stiffer or stronger materials than monolithics but they are tougher, more impact-resistant, and substantially less likely to fail catastrophically.

Typical stress-strain diagrams (Fig. 2) reveal the functional properties of CFCCs, including the linear stress-strain region before matrix failure, matrix cracking, and fiber failure (*11*). The initiation and propagation of matrix cracks are hindered by the presence of the fibers. Energy is absorbed via mechanisms such as fiber debonding and crack deflection that act to improve crack resistance. Upon failure of the matrix, the load is transferred to the fibers. Typically, the first deviation from linear behavior occurs upon matrix cracking, after which the composite is permanently deformed and properties are controlled by the fibers and adhesion and frictional stress at the fiber-matrix interface. Fiber pullout seen in a fracture surface is indicative of the toughening mechanisms (Fig. 2).

Processes in CVI

The primary objectives of CVI are to maximize the rate of matrix deposition and minimize density gradients. Unfortunately, there is an inherent competition between the deposition reaction and the mass transport of the gaseous species. Deposition reactions that are too rapid usually result in severe density gradients, such that essentially complete densification occurs near the external surfaces and much lower densities occur in the interior regions. Alternatively, exceptionally slow deposition reactions require an uneconomically long time to densify the part.

Describing the deposition of matrix material in a porous structure is, in principle, a simple matter. The process is accurately represented by the well-known partial differential equations that describe mass and heat transfer in conjunction with relationships that accurately describe the chemical kinetics and the evolution of the microstructure during infiltration. Because of the practicalities involved in obtaining these specific relationships, the development of fully predictive models has been elusive. For an isothermal, isobaric CVI (ICVI) system, diffusion and a first-order reaction are described by

$$\frac{\partial(\epsilon C)}{\partial t} = \nabla \cdot [\nabla(D_{\mathrm{eff}}C)] - \epsilon S_{\mathrm{v}} k C \quad (2)$$

where ϵ is the void fraction, C is the concentration of the rate-limiting gas-phase reactant, t is time, D_{eff} is the effective diffusion

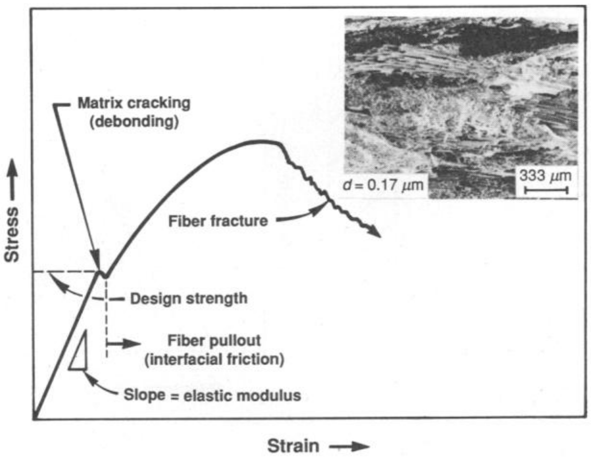

Fig. 2. General stress-strain curve for a fiber-reinforced composite with a scanning electron micrograph showing typical fiber pullout; *d*, interfacial coating thickness.

coefficient of the reactant through the pore structure, k is the first-order rate constant, and S_v is the surface-to-volume ratio of the porosity. The final term is easily modified to describe more complex reaction kinetics. Because the porosity changes as infiltration proceeds, ϵ, S_v, and D_{eff} are not constants. Therefore, the model must also contain additional equations that describe these changes. The complete set of equations can then be solved for appropriate boundary conditions. If mass transport to the outside of the preform is important, then the boundary condition for C at the external surfaces must include a description of this mechanism. The time derivative is usually set to zero, in accordance with the quasi steady-state approximation (*12*).

In the simplest CVI models it is assumed that the process can be treated as a pore diffusion problem with cylindrical pores and a first-order deposition reaction (*13*). This description illustrates how the formation of undesirable density gradients occurs during infiltration. It is convenient to compare the relative deposition and diffusional rates in this process with a dimensionless number called the Thiele modulus, Φ, which represents the ratio between the chemical kinetic deposition rate and the gas-phase mass-transport rate (*14*). The primary difficulty with applying the Thiele modulus to infiltration processes is that its value changes during the process because of changes in pore size. It is therefore convenient to characterize ICVI with the initial value of the Thiele modulus, Φ_0 (*15*). For a first-order deposition reaction in a cylindrical pore,

$$\Phi_0^2 = 2kL^2/r_0D_0 \tag{3}$$

where r_0 and D_0 are the pore radius and the gas diffusivity in the initial preform, respectively, and L is the length of the pore (that is, the characteristic thickness of the preform).

The two limiting cases during ICVI are illustrated in Fig. 3. Under reaction rate–controlling conditions ($\Phi_0^2 << 1$), gas transport is rapid and the initial reactant concentration C_0 is essentially uniform throughout the pore volume. As a result, uniform deposition takes place down the length of the pore, causing no gradient in composite density. For diffusion rate–controlling conditions ($\Phi_0^2 >> 1$), however, the deposition reaction causes a rapidly decreasing concentration of reactants down the pore length, with a proportional decrease in the formation of matrix material and a significant composite density gradient. Mixed control occurs when the two rates are comparable ($\Phi_0^2 \sim 1$).

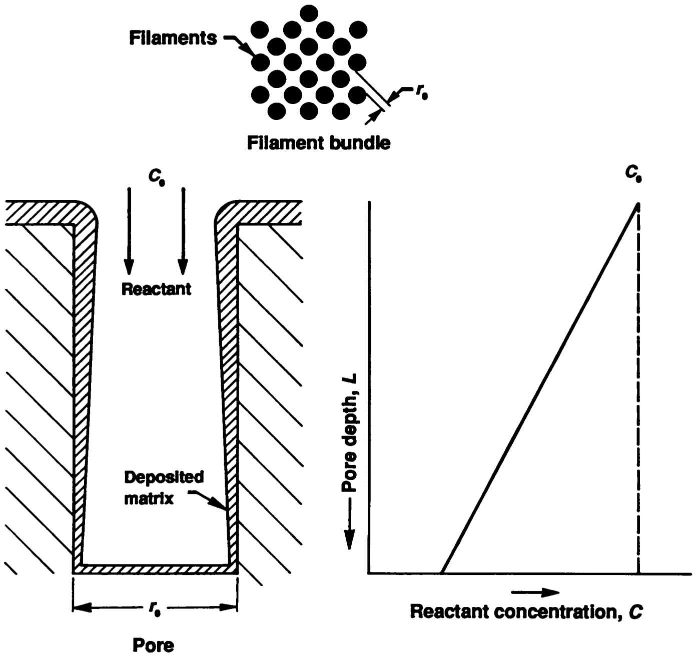

Fig. 3. Reactant and product gas concentrations as a function of axial position down a cylindrical pore: (—) concentration under diffusion rate–limiting conditions; (------) concentration under chemical kinetic rate–limiting conditions.

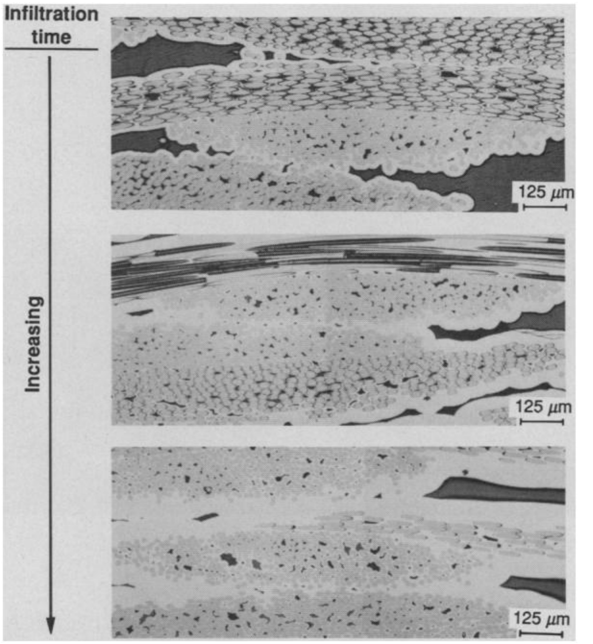

Fig. 4. Polarized light optical photos of polished specimens of Nicalon-SiC composites illustrating pore filling at different stages of the CVI process.

Describing CVI with cylindrical pores does not accurately reflect the often complex microstructures that are present in real preforms. The most common reinforcements in composites formed by CVI are fibers with a relatively small diameter (~10 μm). Bundles of these fibers are woven into cloth layers, which are then stacked to form a preform. In some cases, three-dimensional weaves are also used. All of these preforms have multimodal porosity distributions that range from micrometer scale within fiber bundles to hundreds of micrometers between bundles and cloth layers. The typically anisotropic porosity and fiber architecture govern the gas permeability and the thermal properties. As densification proceeds, the dimensions and distribution of the porosity change nonuniformly with attendant changes in the preform's physical properties. For CVI to be successful, the reactant gases must initially reach the finest porosity (that is, the interfilament volume), react, and fill those pores. When this volume is relatively well infiltrated, the larger interbundle and interply porosity should then be filled. The series of photos in Fig. 4 illustrates this progression during the infiltration of Nicalon fibers with SiC matrix.

Several CVI models have used descriptions of the porosity that are based on the nearly cylindrical shape of the fibers actually used for CVI (*15–18*). Recent efforts to describe the evolving porosity in fibrous preforms are based on Avrami's (*19*) model for phase transformations (*15, 20*). Percolation theory has been used to develop models for reacting porous solids that undergo pore closure, more accurately describing the inevitable formation of trapped porosity (*21–23*). These approaches describe mass transport with percolation in a Bethe lattice (*24*) and can easily be modified to describe CVI (*15*). The primary shortcoming of all of these continuum- and percolation-based models is that they fail to describe the multimodal nature of the porosity in real preforms. However, modeling efforts currently under way are beginning to use multimodal descriptions of the porosity (*25, 26*).

Although work is continuing at several laboratories to develop more extensive CVI models, most of these models have not been successfully applied to experimental results. Thermogravimetric experiments of the reaction-controlled infiltration of fiber bundles with carbon agree generally with the model of Currier and his co-workers (*27*). Sheldon and Besmann (*15*) compared SiC infiltration in individual fiber bundles to modeling results that were based on a first-order reaction. The experimental results showed much poorer infiltration than model predictions that were obtained with a wide variety of descriptions of diffusion. This unfavorable comparison implies that complicated reaction kinetics during SiC deposition from methyltrichlorosilane (MTS) lead to poorer infiltration than a simple first-order reaction. It is theoretically possible that other complex reactions can lead to improved infiltration; calculations based on a sequence of two first-order reactions have been used to demonstrate this possibility (*28, 29*).

Several CVI modeling efforts have described nonisothermal processes (*16, 17, 30*). In these systems, additional complexities are associated with heat transfer and forced convection as infiltration proceeds and the structure of the material changes. For models such as these to accurately describe infiltration behavior, accurate descriptions of the complexities associated with these transport processes will have to be combined with the complex microstructure evolution and chemical kinetics that have already been discussed in connection with ICVI.

Regardless of these complexities and the current inability to fully describe them, understanding the general relationships between the relevant kinetic processes has led to the practical solution of many CVI problems. Temperature control is critical because chemical reactions exhibit Arrhenius behavior such that the rates increase exponentially with temperature. Therefore, relatively low temperatures slow the deposition rate substantially more than diffusion does, thus reducing Φ (*5*). Simple depletion of the reactant gas within the CVI reactor or poisoning of the deposition process by reaction by-products (for example, HCl in the CVI of SiC from MTS) also reduces the deposition rate (*31*). In thermal gradient processes, controlling the temperature difference prevents the entrance surfaces of the gas from becoming sealed until after the interior of the component has reached an acceptable density (*7*).

CVI Techniques

There are five general classes of CVI techniques (Fig. 5): type I, isothermal; type II, thermal gradient; type III, isothermal-forced flow; type IV, thermal gradient–forced flow; and type V, pulsed flow. The most widely used commercial process is type I, ICVI (*5, 6, 32*). ICVI depends on only diffusion for species transport and generally operates at reduced pressure (1 to 10 kPa) for deposition rate control. Fixturing (mechanical restraint) of the fibrous preforms is needed before initial densification to maintain the proper shape. Density gradients are minimized by a low reaction temperature although, to obtain economical densification rates, deposition is often sufficiently rapid to overcoat the outer surface before infiltration is complete. Interruption of the CVI process for periodic machining is thus necessary for all but the thinnest parts to open diffusion paths from the surface. Regardless, this diffusion-dependent process is still slow, requiring several weeks for infiltration. It is commercially attractive, however, because large numbers of parts of varying dimensions are easily accommodated in a single reactor.

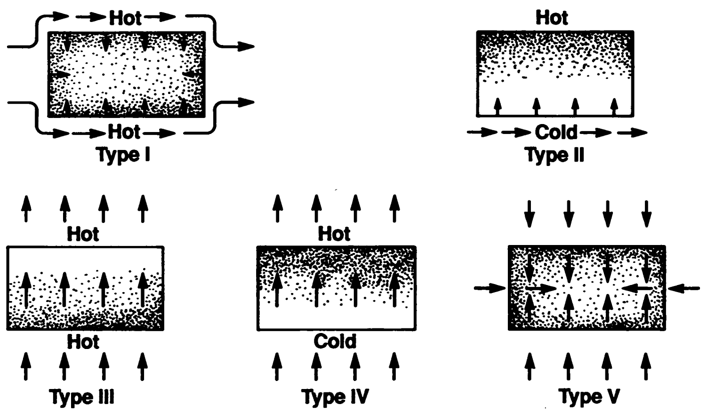

Fig. 5. The five general classes of CVI techniques. Type 1, isothermal: reagents surround preform and transport to the interior via diffusion (ICVI). Type 2, thermal gradient: reagents contact cold surface of preform and also transport by diffusion. Type III, isothermal–forced flow: reagents flow through preform. Type IV, thermal gradient–forced flow: reagents flow through preform from cold to hot surface (FCVI). Type V, pulsed flow: reagents flow into and out of preform because of cyclical evacuation and backfilling. [Adapted from (*41*) with permission of the Electrochemical Society, copyright 1990]

The thermal gradient and isothermal–forced flow processes (types II and III) appear to be little used but may have advantages under certain circumstances. The thermal gradient process is relatively slow because it also depends on diffusion; however, sealing of the entrance surface is prevented by maintaining the surface at low temperature. As densification approaches completion, the temperature of the cooler surface rises as a result of the greater conductivity of the denser region, causing infiltration of the entire volume. The potentially more rapid isothermal–forced flow processes, which uses forced convection, suffers from density gradients and loss of permeability at the entrance surface, as is seen also in the isothermal process. The forced-flow–thermal gradient technique (FCVI) (type IV) developed at Oak Ridge National Laboratory overcomes the problems of slow diffusion and restricted permeability and is capable of producing thick-walled, simple-shaped components in times on the order of hours (*7, 8*). All of these techniques require individual fixturing of each part to maintain the required shape and pressure or thermal gradients.

Pulsed-flow CVI (type V) utilizes alternate introduction of reactant gases and evacuation of the CVI reactor to rapidly transport reactant species into, and product gases out of, the preform (*33–35*).

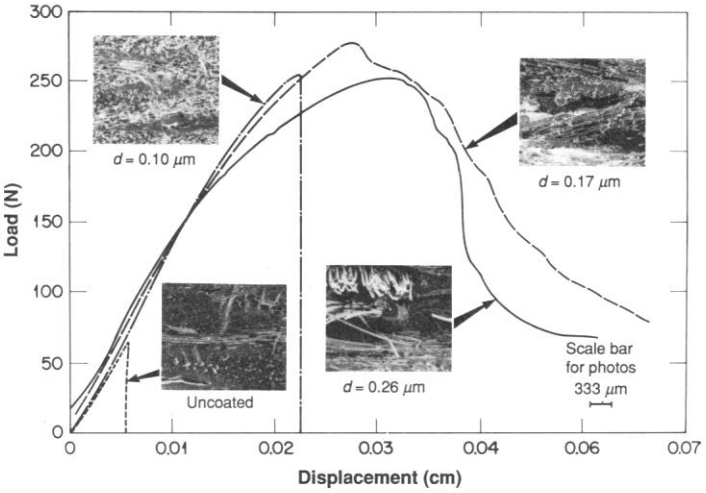

Fig. 6. Effect of the thickness of the pyrolytic carbon interlayer on the mechanical properties of the composite. The greater toughness seen in the load-displacement curves corresponds to increased fiber pullout seen in the scanning electron micrographs of the respective fracture surfaces.

The technique has not been widely investigated, although some modeling calculations indicate that it can significantly improve infiltration rates over those experienced in ICVI *(35)*.

The ICVI and FCVI processes currently attract the most commercial interest. Advantage may be gained by using different conditions to infiltrate the coarser porosity in a preform, after the finer porosity is filled, to deposit significant amounts of material in these larger volumes within reasonable time. In ICVI, the conditions (temperature or gas concentration) can be explicitly changed, and, as a result, the process occurs in several steps. For large reactors, the initial infiltration is likely achieved by placing the preform in the region of the furnace that is at a lower temperature or where it will contact only significantly depleted reactant gases (downstream regions). As the finer porosity becomes filled, the parts may be moved to regions of higher temperature or lower gas depletion to more rapidly fill the coarser porosity. During these interruptions of the process, surface grinding can be performed to reopen channels for diffusion. It is not possible, however, to produce fully dense material; in cloth lay-up preforms, for example, the lower limit of the void fraction is ~10%.

The FCVI process is self-optimizing, which has allowed for much shorter infiltration times and less difficulty in obtaining uniform infiltration. The furnace is configured to apply a thermal gradient across the preform, in part by actively cooling the entrance surface of the reactant gas. As expected, the preform is infiltrated most rapidly near the hot surface with a diffuse densification front moving from the hot surface toward the cooled entrance surface. Infiltration of the finer porosity must, again, occur during the initial infiltration period under conditions where $\Phi << 1$ for the micrometer-scale radii. For the volume near the cooled surface Φ is minimized by the low temperature, whereas nearer the hot surface it is forced to small values by depletion of reactants.

As the finer porosity is filled and the density of the part increases, its thermal conductivity increases and the thermal gradient decreases. The temperatures across the part are generally higher, increasing Φ and allowing coarser porosity to be efficiently filled with matrix. Thus, in a self-controlled manner, the various scales of porosity are progressively filled. Infiltration is typically assumed to be complete when permeability is diminished such that the pressure drop across the part becomes prohibitive (70 to 140 kPa). Intermediate surface grinding is not necessary in this process, although it often is in ICVI, and the process can continue uninterrupted to final density. Some finishing may be necessary, however, to remove pieces of fixturing or to smooth surfaces.

Fibrous Preforms

Fibers. The properties of the fibers in CFCCs are fundamental to the properties of the composites. Like the matrix, the fibers have high strength with a high elastic modulus. Although an advantage of CVI processing is prevention of damage to ceramic fibers, they must still be able to withstand the CVI environment. This generally entails elevated temperatures of the order of 1000°C and corrosive matrix precursors.

Several oxide, carbide, and nitride fibers that offer a variety of properties to the material designer (Table 1) have become available in recent years *(36)*. However, almost all have been restricted to developmental activities. Silicon carbide fibers are attractive for use in high-temperature, oxidative environments and are being established in commercial products. A chemical vapor–deposited, large-diameter (~150-μm) SiC fiber has been used in CVI, but such a large fiber is difficult to form into other than very simple shapes. The most commonly used SiC fiber is Nicalon, a polymer-derived microcrystalline/amorphous material containing significant amounts of silica. A newer and possibly higher strength fiber (Tyranno) has also become available. Oxide fibers have seen somewhat more limited application, with a series of amorphous aluminosilicate fibers and polycrystalline alumina-based fibers, which are noted for their high purity, being investigated.

In general, the polymer-derived, amorphous fibers, although they have the advantage of lower cost and easier handling, typically lose strength at elevated temperatures and in CVI environments *(1, 2)*. The crystalline fibers, unfortunately, are typically costly and have lower room-temperature strengths.

Preforms. Preform geometries can be tailored to the application to maximize strength and toughness in the direction of maximum stresses. The general types of preforms include felts, which are continuous fiber lengths that are randomly oriented and maintained in shape by entanglement. A common preform is made by stacking layers of tape (for unidirectional reinforcement) or cloth plies (for reinforcement within the plane of the cloth). The most sophisticated preforms are three-dimensional weaves or braids, which can offer multidimensional reinforcement bordering on isotropy.

Matrix Materials

A large variety of matrix materials have been used to produce CFCCs by CVI: SiC, B_4C, TiC, HfC, Si_3N_4 (amorphous), AlN, TiB_2, Al_2O_3, and ZrO_2. This list could be easily extended to include

Table 1. Properties of some commercially available fibers. Information was obtained, in part, from *(36)*.

Manufacturer	Designation	Composition (% by weight)	Tensile strength (MPa)	Tensile modulus (GPa)	Density (g/cm^3)	Diameter (μm)
Avco	SCS-6	SiC on carbon core	3920	406	3.0	143
Avco		Si, C	>2800	280–315		6–10
Dow Corning–Celanese	MPDZ	47 Si, 30 C, 15 N, 8 O	1750–2100	175–210	2.3	10–15
Dow Corning–Celanese	HPZ	59 Si, 10 C, 28 N, 3 O	2100–2450	140–175	2.35	10
Dow Corning–Celanese	MPS	60 Si, 30 C, 1 O	1050–1400	175–210	2.6–2.7	10–15
DuPont	FP	>99 α-Al_2O_3	>1400	385	3.9	20
DuPont	PRD-166	Al_2O_3, 15–25 ZrO_2	2100–2450	385	4.2	20
Nippon Carbon	Nicalon	59 Si, 31 C, 10 O	2520–3290	182–210	2.55	10–20
Sumitomo		85 Al_2O_3, 15 SiO_2	1800–2600	210–250	3.2	9–12
3M	Nextel 312	62 Al_2O_3, 14 B_2O_3, 24 SiO_2	1750	154	2.7	11
3M	Nextel 440	70 Al_2O_3, 28 SiO_2, 2 B_2O_3	2100	189	3.05	10–12
3M	Nextel 480	70 Al_2O_3, 28 SiO_2, 2 B_2O_3	2275	224	3.05	10–12
Ube	Tyranno	Si, Ti, C, O	>2970	>200	2.3–2.5	8–10

many other ceramics that can be deposited via a CVD reaction, including even complex systems such as the new, high-temperature superconductors. Integrated circuit substrates with directionally controlled thermal conductivities could be produced with fibers and matrix properly oriented. It is not required that the matrix be single phase, because composite coatings by CVD have been demonstrated and, thus, multiple-phase matrices are theoretically possible. With such composite matrices, the CFCC toughness may be further enhanced. Currently, however, the only commercial materials available are those with a SiC matrix.

Fiber-Matrix Interface

Interfacial shear stresses play a key role in determining the mechanical properties of a fiber-reinforced ceramic composite. In single-phase materials, the energy absorbed during fracture is determined by the applied forces and the strain and surface energies of that material. Composites, however, involve the additional phenomena of strain energy of the fibers and the work done in debonding the fibers from the matrix. These additional factors will increase the stress at which the matrix in a composite will begin to crack.

Experience has shown that Nicalon and most other fibers require precoating before infiltration to avoid strong interfacial bonding, low flexure strength, and brittle fracture (Fig. 6). Composites with uncoated fibers exhibit fracture surfaces that are flat and smooth with no evidence of fiber pullout and result in little toughening. To control the mechanical properties of Nicalon-SiC composites, a thin pyrolytic carbon layer is deposited on fibrous preforms before densification to provide a controlled and uniform interface with the matrix. The carbon deposition conditions are chosen to produce a graphitic coating with a laminar structure that lies parallel to the fibers (*37, 38*). The coating prevents chemical damage of the fibers during processing and prevents weakening of the fiber-matrix interface, enhancing fiber debonding and slip (*39, 40*). Thus, the coating results in an increase in the toughness and the ultimate strength of the composite materials. Recent work on alternative, more oxidation-resistant coatings have indicated that hexagonal BN may usefully replace carbon.

Conclusions

CVI can be an efficient process for producing CFCCs with extremely attractive properties. Their refractory character coupled with the directionally controlled strength and toughening result in a new class of materials available for unique applications. In the near term, these CFCCs will likely be used in high-value applications because of their current high cost and limited availability. Larger markets are expected to open as the processing technology matures, lowering the price and providing greater variety of geometries, fibers, and matrices.

Much work remains to be done on the efficient fabrication of CFCCs by CVI. The level of effort in modeling the complex processes has grown severalfold over only the last 3 years, and potentially useful models are now appearing. These models need to be confirmed or modified with experimental corroboration. For the models to be useful, they must follow densification in real time; thus, sensor systems for large-scale CVI reactors will need to be implemented.

Finally, the opportunity CVI provides to produce multicomponent materials is far from fully explored. Systems can be developed with multiple-fiber types providing directionally different properties (for example, high thermal conductivity in only one plane for thermal protection and efficient heat removal). Multiple-phase matrices can further increase toughness and may also improve properties such as oxidation behavior. The CVI processes have progressed to an emerging technology, the limits of which are yet to be fully understood.

REFERENCES AND NOTES

1. G. Simon and A. R. Bunsell, *J. Mater. Sci.* **19**, 3658 (1984).
2. P. J. Lamicq, G. A. Bernhart, M. M. Dauchier, J. G. Mace, *Am. Ceram. Soc. Bull.* **65** (no. 2), 336 (1986).
3. R. L. Bickerdike, A. R. G. Brown, G. Hughes, H. Ranson, in *Proceedings of the Fifth Conference on Carbon*, S. Mrosowski, M. C. Studebaker, P. L. Walker, Eds. (Pergamon, New York, 1962), vol. 1.
4. W. C. Jenkin, U.S. Patent 3,160,517 (8 December 1964).
5. E. Fitzer and R. Gadow, *Am. Ceram. Soc. Bull.* **65** (no. 2), 326 (1986).
6. R. Naslain and F. Langlais, *High Temp. Sci.* **27**, 221 (1990).
7. D. P. Stinton *et al.*, *Am. Ceram. Soc. Bull.* **67** (no. 2), 350 (1988).
8. T. M. Besmann *et al.*, *Mater. Res. Soc. Bull.* **13** (no. 11), 45 (1988).
9. *Materials Science and Engineering for the 1990s: Maintaining Competitiveness in the Age of Materials* (National Academy Press, Washington, DC, 1989).
10. A. G. Evans, *J. Am. Ceram. Soc.* **73** (no. 2) 187 (1990); J. A. Cornie, A. S. Argon, V. Gupta, *Mater. Res. Soc. Bull.* **16** (no. 4), 32 (1991).
11. J. J. Mecholsky, *Am. Ceram. Soc. Bull.* **65** (no. 2), 315 (1986).
12. D. Luss, *Can. J. Chem. Eng.* **46**, 154 (1968).
13. C. H. J. Van den Brekel, R. M. M. Fonville, P. J. M. Van der Straten, G. Verspui, in *Proceedings of the 8th International Conference on CVD*, Paris, J. M. Blocher *et al.*, Eds. (Electrochemical Society, Pennington, NJ, 1981), pp. 142–156.
14. E. W. Thiele, *Ind. Eng. Chem.* **31**, 916 (1939).
15. B. W. Sheldon and T. M. Besmann, in preparation.
16. N.-H. Tai and T.-W. Chou, *J. Am. Ceram. Soc.* **73**, 1489 (1990).
17. T. L. Starr, *Ceram. Eng. Sci. Proc.* **9**, 803 (1988).
18. R. P. Currier, *J. Am. Ceram. Soc.* **73**, 2274 (1990).
19. M. Avrami, *J. Chem. Phys.* **8**, 212 (1940).
20. R. P. Currier, in *Proceedings of the 11th International Conference on CVD*, Seattle, G. W. Cullen and K. E. Spear, Eds. (Electrochemical Society, Pennington, NJ, 1990), pp. 492–498.
21. Y. C. Yortsos and M. M. Sharma, *Am. Inst. Chem. Eng. J.* **32**, 46 (1986).
22. H. C. Yu and S. V. Sotirchos, *ibid.* **33**, 382 (1987).
23. S. Reyes and K. F. Jensen, *Chem. Eng. Sci.* **42**, 565 (1987).
24. M. Sahimi, G. R. Gavalas, T. T. Tsotsis, *ibid.* **45**, 1443 (1990).
25. T. L. Starr and A. W. Smith, in preparation.
26. B. W. Sheldon and T. M. Besmann, in preparation.
27. D. J. Devlin, R. S. Barbero, R. P. Currier, in *Proceedings of the 11th International Conference on CVD*, Seattle, G. W. Cullen and K. E. Spear, Eds. (Electrochemical Society, Pennington, NJ, 1990), pp. 499–505.
28. S. Middleman, *J. Mater. Res.* **4**, 1515 (1989).
29. B. W. Sheldon, *ibid.* **5**, 2729 (1990).
30. T. L. Starr and A. W. Smith, in *Chemical Vapor Deposition of Refractory Metals and Alloys*, T. M. Besmann and B. M. Gallois, Eds. (Materials Research Society, Pittsburgh, 1990), pp. 55–60.
31. T. M. Besmann, B. W. Sheldon, M. D. Kaster, in preparation.
32. J. Y. Rossignol, F. Langlais, R. Naslain, in *Proceedings of the 9th International Conference on CVD*, Cincinnati, McD. Robinson *et al.*, Eds. (Electrochemical Society, Pennington, NJ, 1984), pp. 596–614.
33. R. L. Beatty and D. V. Kiplinger, *Nucl. Appl. Technol.* **8** (no. 6), 488 (1970).
34. K. Sugiyama and E. Yamamoto, *J. Mater. Sci.* **24**, 3756 (1989).
35. S. V. Sotirchos and M. M. Tomadakis, in *MRS Symposium Proceedings on Chemical Vapor Deposition of Refractory Metals and Ceramics*, T. M. Besmann and B. M. Gallois, Eds. (Materials Research Society, Pittsburgh, 1989), pp. 73–80.
36. L. M. Sheppard, *Am. Ceram. Soc. Bull.* **69** (no. 4), 670 (1990).
37. W. V. Kotlensky, *Chem. Phys. Carbon* **9**, 173 (1973).
38. H. O. Pierson and M. L. Lieberman, *Carbon* **13**, 159 (1975).
39. R. A. Lowden, *Publ. ORNL/TM-11039* (Oak Ridge National Laboratory, Oak Ridge, TN, 1989).
40. R. A. Lowden and K. L. More, in *MRS Symposium Proceedings on Interfaces in Composites*, C. G. Pantano and E. J. H. Chen, Eds. (Materials Research Society, Pittsburgh, 1989), pp. 205–214.
41. T. M. Besmann, R. A. Lowden, B. W. Sheldon, D. P. Stinton, in *Proceedings of the 11th International Conference on CVD*, Seattle, G. W. Cullen and K. E. Spear, Eds. (Electrochemical Society, Pennington, NJ, 1990), pp. 482–491.

42. We thank K. L. More, T. N. Tiegs, D. F. Craig, and R. R. Judkins for valuable comments. We thank W. J. Lackey who provided a model for Fig. 5. We thank J. I. Kelly for manuscript preparation and H. R. Livesey for the graphics. Supported by the U.S. Department of Energy, Fossil Energy Advanced Research and Technology Development Materials Program, under contract DE-AC05-84OR21400 with Martin Marietta Energy Systems, Inc.